Anomalous High Pressure Dependence of the Jahn-Teller Phonon in $La_{0.75}Ca_{0.25}MnO_3$

A. Congeduti,[1] P. Postorino,[1] E. Caramagno,[2] M. Nardone,[2] A. Kumar,[3] and D. D. Sarma[3]

[1]*Dipartimento di Fisica, Università di Roma "La Sapienza," Unità dell'Istituto Nazionale per la Fisica della Materia Piazzale Aldo Moro 2, 00185 Roma, Italy*

[2]*Dipartimento di Fisica, Università di Roma Tre, Unità dell'Istituto Nazionale per la Fisica della Materia Via della Vasca Navale 84, 00146 Roma, Italy*

[3]*Solid State and Structural Chemistry Unit, Indian Institute of Science, Bangalore 560012, India*

Raman spectra of $La_{0.75}Ca_{0.25}MnO_3$ have been collected for the first time over a wide pressure range (0−14 GPa) using a diamond anvil cell. The frequency range explored (200−1100 cm^{-1}) and the very good quality of the data allowed us to carefully analyze the pressure evolution of the phonon modes of the MnO_6 octahedra. The results show an abrupt transition at ∼7.5 GPa with an evident deviation from the linear trend of the frequency of the Jahn-Teller phonon versus the applied pressure, accompanied by a strong phonon broadening. This behavior disagrees with the predicted insulator to metal transition and, on the contrary, indicates the occurrence of a new unpredicted phase in the very high pressure regime.

The $A_{1-x}A'_xMnO_3$ pseudocubic manganese perovskites (A is a rare earth and A' is a divalent cation) have been the subject of extended investigations because of either the potential technological applications or the basic interest in solid state physics. As a matter of fact, the phase diagram of these compounds is particularly rich and many variables such as pressure, applied magnetic field, doping concentration x, A-site average ionic radius $r_A = x_A R_A + x_{A'} R_{A'}$ (where R_A is the A-ion radius) can determine the different phases of the system [1]. At ambient pressure the T vs x phase diagram of La-Ca manganites shows two phases in the $0.2 < x < 0.5$ Ca concentration range: a paramagnetic insulating phase above T_C and a ferromagnetic metallic phase below [2]. The occurrence of the insulator to metal (IM) transition is governed by the balance between two competing effects: the "double exchange" magnetic interaction [3], which increases the electron kinetic energy and hence delocalization, and the strong Jahn-Teller (JT) coupling which tends to localize the carrier in a local lattice distortion [4]. Diffraction measurements, performed as a function of temperature, have shown that the large JT distortion of the MnO_6 octahedra in the insulating state reduces to vanishingly small values at the IM transition [5]. The interplay between charge localization and octahedra distortion has been found also when the metallic phase is approached by varying other parameters. In the T vs r_A phase diagram, at constant electronic doping x, the increase of r_A produces indeed both a reduction of the octahedra distortion and an enhancement of the metallic character. With $x = 0.3$, T_C increases by about 200 K going from $r_A = 1.19$ Å to $r_A = 1.24$ Å [6,7]. In principle a reduction of the JT distortion could also be obtained by applying an external pressure. Actually an increase of T_C was observed as the pressure is increased [8,9]. The comparison between the effects on T_C of the "internal pressure" (determined by r_A) and of the external pressure yields an empirical conversion factor $r_A/P = 3.7 \times 10^{-3}$ Å/GPa in the 0–1.5 GPa range [8]. The underlying idea is that an IM transition occurs if a sufficient reduction of the "free volume" around the A site is obtained, i.e., if the octahedra are forced to be undistorted and the Mn-O-Mn angle tends to 180° [8,10]. This can be achieved either by increasing the average dimension of the atom at the A site (internal pressure) or by contracting the cage of the MnO_6 octahedra (external pressure). This guess has been proved in a relatively small pressure range [8,9] whereas there is no experimental indication that it holds also in the very high pressure regime. Within this scheme and taking into account the r_A/P conversion factor, the room temperature metallization pressure for $La_{0.75}Ca_{0.25}MnO_3$ can be estimated as $P_{IM} \approx 5$ GPa. From a spectroscopic point of view, the signature of the IM transition can be identified by a significant narrowing and frequency hardening of the octahedron bending and stretching modes, as pointed out by both theoretical and experimental investigations [11–13]. These effects are direct consequences of the charge-lattice coupling reduction and of the free carrier screening in the metallic phase. Raman spectroscopy is therefore an ideal tool for studying these materials, and it is particularly suitable for high pressure studies. Several papers have been published in the last few years [13–16], but there is a complete lack of experimental data as a function of pressure. With the idea of searching for a pressure-driven IM transition, Raman spectra of a polycrystalline $La_{0.75}Ca_{0.25}MnO_3$ sample have been collected over a wide pressure range (0–14 GPa) using a membrane diamond anvil cell (MDAC).

Raman spectra were measured in back-scattering geometry, using a micro-Raman spectrometer (LABRAM by Dilor) with a charge-coupled device (CCD) detector and an adjustable notch filter. The sample was excited by the 632.8 nm line of a 16 mW He-Ne Laser. The confocal microscope was equipped with a 20× magnification

objective which gives laser spot about 10 μm^2 wide at the sample surface. The notch filter cutoff at low frequency and the very intense diamond Raman peak at high frequency (1331 cm^{-1} at zero pressure) limited the reliability of the spectra outside the 200–1100 cm^{-1} frequency range. The MDAC (by BETSA) was equipped with low fluorescence IIA diamonds with 800 μm culet diameter, the gaskets were made of a 250 μm thick steel foil (AISI 301). Under working conditions the gasket thickness was ranging from 30 to 50 μm with a typical 200 μm diameter hole. Polycrystalline samples of the orthorhombic (*Pnma*) $La_{0.75}Ca_{0.25}MnO_3$ manganite were prepared by a standard solid state reaction method and characterized by x-ray diffraction, EXAFS spectroscopy, ac susceptibility, and resistivity measurements [17,18]. In particular, the magnetoresistance curve reported in Ref. [18] shows a quite narrow and intense peak around T_C. By finely milling the sample, we obtained a powder with an average grain size of the order of 1 μm. Manganite grains were then placed in the center of the top surface of an NaCl pellet, obtained by synthesizing salt powder at high pressure directly within the gasket hole. Few ruby nanospheres were also placed around and over the manganite sample in order to measure the pressure through the standard ruby fluorescence technique [19]. We verified that pressure gradients, if any, were within the experimental uncertainty of ~0.2 GPa. The loading procedure we adopted ensures hydrostatic conditions for the sample grains and, owing to the high thermal conductivity of diamond, prevents spurious effects due to laser-induced sample heating [14,15]. A complete reproducibility of the spectra was obtained on releasing the pressure on the sample.

Raman spectra were collected from five different points of the sample. Since the laser spot impinges only a few sample grains, the relative intensities of the peaks were slightly different from point to point depending on the average orientation of the grains. Therefore the spectra were analyzed separately and the best fit parameters were averaged for each pressure. In Fig. 1 the Raman spectrum collected at 2 GPa is shown. Four broad phonon peaks are well evident in the 200–800 cm^{-1} spectral region and a weak structure, ascribed to electronic scattering, is present around 1000–1100 cm^{-1}. The strong rise of the intensity on the high frequency side is due to the diamond Raman peak. Spectra were fitted in the 200–1100 cm^{-1} frequency range with the function [13]

$$S(\nu) = [1 + n(\nu)]\left[\frac{A\nu\Gamma}{\nu^2 + \Gamma^2} + \sum_{i=1}^{5}\frac{A_i\nu\Gamma_i}{(\nu^2 - \nu_i^2)^2 + \nu^2\Gamma_i^2}\right]. \quad (1)$$

The first term represents the low frequency electronic (LFE) Raman scattering due to diffusive hopping of the carriers. The sum, in the second term, is meant to account for both the four phonon peaks and the high frequency electronic (HFE) contribution (ν_i, A_i, and Γ_i are the peak frequency, amplitude, and linewidth, respectively). The quantity $n(\nu)$ is the Bose-Einstein thermal population factor. The agreement between the experimental data and the fitting curve was quite good at all the investigated pressures. As an example the best fit curve and the different components are also shown in Fig. 1.

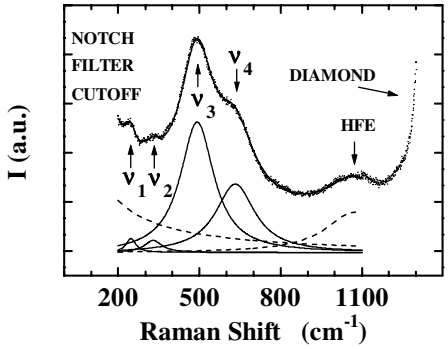

FIG. 1. The Raman spectrum at 2 GPa of $La_{0.75}Ca_{0.25}MnO_3$ and the best fit curve from Eq. (1) (solid line) are shown. The four phonon contributions (solid lines) and the electronic contributions LFE and HFE (dashed lines) are also shown separately.

Raman spectra collected at different pressures from a given point of the sample are shown in Fig. 2. The pressure dependence of the LFE and HFE responses could not be thoroughly analyzed owing to the spectral range limitation discussed above. Nevertheless, as far as the HFE peak is concerned, we can at least exclude that a significant softening of its peak frequency occurs as the pressure

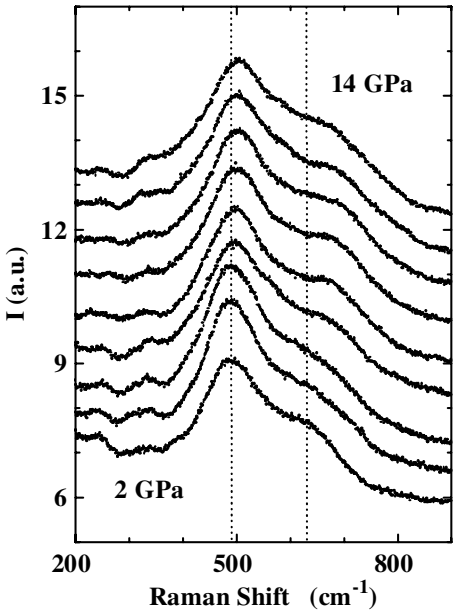

FIG. 2. The Raman spectra of $La_{0.75}Ca_{0.25}MnO_3$ at different pressures. The pressure increases from bottom to top from 2 to 14 GPa. The zero pressure frequencies of ν_3 and ν_4 phonons are shown as vertical dotted lines.

is increased. In Ref. [13] it was suggested that this contribution should be associated with the photoionization of small polarons. In particular, a remarkable softening of the peak frequency was observed with decreasing temperature [13], when the metallic phase is approached and the polaron binding energy is consequently decreased. On the basis of this suggestion, our results on the HFE peak exclude the occurrence of a pressure induced metallization over the whole explored pressure range.

Comparing the present data with the assignments reported in Ref. [15], the four observed phonon peaks [$\sim$240 cm^{-1} (ν_1), $\sim$330 cm^{-1} (ν_2), $\sim$480 cm^{-1} (ν_3), $\sim$630 cm^{-1} (ν_4) at zero pressure] can be ascribed to the octahedron modes $A_g(2)$ (b-axis rotation), $B_{3g}(4)$ (c-axis rotation), $A_g(3)$ (apical oxygen bending), and $B_{2g}(1)$ (in-plane oxygen stretching), respectively. The pressure dependence of the phonon frequencies is shown in Fig. 3a. The frequency ν_1 is almost unaffected by pressure as expected for a b-axis rotation, and this mode has been demonstrated to be nearly independent of both transport and magnetic properties [14]. On the contrary, ν_2 shows an abrupt hardening around $P^* \sim 7.5$ GPa with a total frequency shift of 30 cm^{-1}. The bending phonon frequency ν_3 shows a weak, roughly linear pressure dependence, while the stretching phonon frequency ν_4 shows a strong linear increase up to P^* followed by a saturation around 680 cm^{-1}. The stretching mode ν_4 is the most sensitive to pressure with a slope of 6.4 cm^{-1}/GPa in the $0-P^*$ range (see Fig. 3a). In the same pressure range, almost identical frequency values and slope were found for the higher frequency mode in $La_{0.5}Sr_{1.5}MnO_4$ layered manganite for which, however, the linear trend continues up to 14 GPa [20]. This is a JT phonon in both layered (general formula $A_xA'_{2-x}MnO_4$) and pseudocubic manganites. The saturation effect found for the latter system must be related to some abrupt change of the JT distortion. The different high pressure behavior of the two manganites can be ascribed to the different extent of A trapping [21]. Indeed, in the layered manganite the element at the A site is inserted between disconnected planes of MnO_6 octahedra, whereas it is completely trapped within the strongly connected 3D octahedra cage in the pseudocubic manganite. The present phonon frequency pressure dependence and the compressibility evaluated by diffraction data [17] allowed us to calculate the Gruneisen parameter values given by $\gamma_i = -\partial \ln(\nu_i)/\partial \ln(V)$. In the $0 - P^*$ pressure region we found $\gamma_1 \simeq \gamma_2 < 1$, $\gamma_3 \simeq 1$, and $\gamma_4 \simeq 2$. These values support the proposed assignment of the phonon modes. Indeed, a value $\gamma > 1$ is frequently encountered for internal stretching modes, while $\gamma \leq 1$ is characteristic of external molecular modes such as rigid rotation modes.

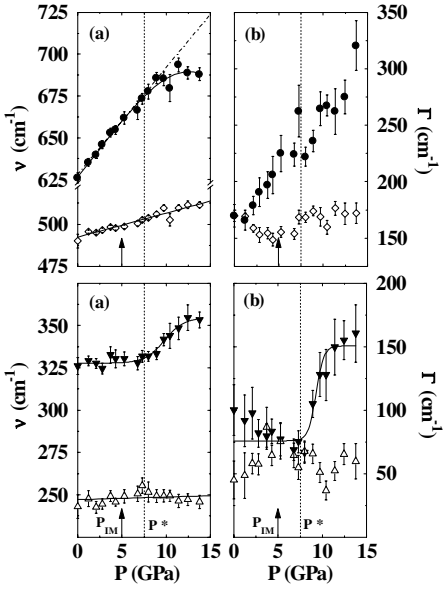

FIG. 3. Pressure dependence of frequencies (a) and linewidths (b) for the four phonon peaks: ν_1 (up triangles), ν_2 (down triangles), ν_3 (diamonds), ν_4 (circles). The dash-dotted line in the (a) upper panel is the linear fit of ν_4 frequencies in the $0-P^*$ pressure range. Vertical dashed lines indicate $P^* = 7.5$ GPa, arrows $P_{IM} = 5$ GPa. Solid lines are a guide for the eye.

As far as the phonon profile is concerned, it is worth noticing that the presence of a strong coupling shortens the phonon lifetime and consequently broadens the phonon widths. Indeed the linewidths observed in the JT undistorted end-member $CaMnO_3$ are almost 1 order of magnitude narrower [14,20] than those of doped samples [20,22]. Moreover, an abrupt 30% narrowing of the Raman peaks was observed below T_C [13], where the JT octahedra distortion vanishes. In Fig. 3b the pressure dependence of the phonon linewidths is shown. While the widths Γ_1 and Γ_3 are almost pressure independent (apart, maybe, from a small discontinuity of Γ_3 around P^*), both Γ_2 and Γ_4 show a strong increase with the pressure. In particular, this increase appears as an abrupt broadening around P^* for the octahedra rotation mode (Γ_2), while it is more gradual, albeit more substantial, for the stretching mode (Γ_4) where it results as high as 100%.

The above results disagree with the hypothesis of the occurrence of a pressure induced IM transition: neither the phonon frequencies and widths nor the HFE contribution shows the expected behavior for a metallization transition [11,13]. On the contrary, the pressure behavior of the stretching and rotational modes in the two pressure regions $P < P^*$ and $P > P^*$ suggests a different interpretation. Lattice compression strongly and steadily hardens the frequency of the stretching mode ν_4 in the $P < P^*$ region. The Mn-O-Mn angle is expected to increase towards the ideal 180° value of the cubic structure, so that a consequent increase of the bandwidth and of the metallic character of the system would occur. However, a real metallic phase is not achieved: the observed remarkable pressure-driven increase of the Γ_4 width is in contrast with a charge delocalization. At the same time pressure hardly affects the rotation frequency of the MnO_6 octahedra

indicating that these are not being severely distorted and/or reoriented by pressure. However, this effect shows up in the abrupt variations in frequency and linewidth observed for ν_2 at P^* and it may correspond to a new equilibrium position for the octahedra. This is not an IM transition since it would imply a further stiffening of the stretching mode ν_4 as well as a reduction of the corresponding damping whereas the opposite behavior was observed. Finally, the unusually weak pressure dependence of the phonon frequencies (particularly of the JT mode ν_4) in the $P > P^*$ pressure region suggests that the structural and/or charge arrangement is in progress as also confirmed by the observed progressive redistribution of the intensities between ν_3 and ν_4 in favor of the high frequency one [23]. These findings, together with the continuous increase of all the phonon widths as a function of increasing pressure, suggest that the charge-lattice interaction is strengthened by the lattice compression. The presence of an anomaly in the pressure dependence of our sample's structure and the guess of an increased role played by lattice-charge interaction are in agreement with the results of a recent high pressure experiment, where an abrupt and huge increase of the JT distortion of the octahedra has been found around P^* [17]. We want to stress that our conclusions are not in contrast with the previous results where a reduction of the electron-phonon coupling as a function of increasing pressure was claimed [9]. The experimental data in Ref. [9] refers to a small pressure region (0–1.1 GPa) and the observed increase of T_C is consistent with the hardening of the ν_4 stretching mode that we observe in the $P < P^*$ region. At present we are not able to give a satisfactory explanation of the experimental findings in the high pressure regime although it is evident that, besides steric effects, some other elements (such as configurational disorder [2,7], magnetic interactions) should be taken into account. We can guess indeed that the saturation effect shown by the JT phonon could originate from the onset at P^* of a pressure activated mechanism which enters into competition with the hardening due to the lattice compression dominant in the $P < P^*$ pressure range. In this context can be noticed the recently observed softening of the JT mode at the onset of the antiferromagnetic order in $LaMnO_3$ [22,24].

The Raman measurements reported in the present Letter provide the first high pressure (0–14 GPa) spectroscopic data on manganites. The very good quality of the Raman spectra allowed us to carefully determine the pressure dependence of four octahedra phonon modes. No spectroscopic evidence for the IM transition, expected on the basis of the correspondence between internal and external pressures, was found. On the contrary, the abrupt discontinuity observed in both frequency and width versus pressure at $P^* = 7.5$ GPa can be seen as an indication of the onset of a new unpredicted phase which seems to persist up to 14 GPa.

We would like to acknowledge C. Meneghini for making available the structural data under pressure prior to publication. We also acknowledge P. Dore and S. Lupi for fruitful discussion and helpful comments.

[1] A. J. Millis, Nature (London) **392**, 147 (1998); J. Fontcuberta, Phys. World **12**, 33 (1999).
[2] S-W. Cheong and H. Y. Hwang, in *Colossal Magnetoresistance Oxides,* edited by Y. Tokura, Monographs in Condensed Matter Science (Gordon and Breach, Reading, U.K., 2000).
[3] C. Zener, Phys. Rev. **82**, 403 (1951).
[4] A. J. Millis, P. B. Littlewood, and B. I. Shraiman, Phys. Rev. Lett. **74**, 5144 (1995); A. J. Millis, B. I. Shraiman, and R. Mueller, Phys. Rev. Lett. **77**, 175 (1996).
[5] P. G. Radaelli *et al.,* Phys. Rev. B **56**, 8265 (1997); P. G. Radaelli *et al.,* Phys. Rev. B **54**, 8992 (1996).
[6] H. Y. Hwang *et al.,* Phys. Rev. Lett. **75**, 914 (1995).
[7] J. Foncuberta, V. Laukhin, and X. Obradors, Appl. Phys. Lett. **72**, 2607 (1998).
[8] H. Y. Hwang *et al.,* Phys. Rev. B **52**, 15 046 (1995).
[9] V. Laukhin *et al.,* Phys. Rev. B **56**, R10 009 (1997).
[10] J. L. Garcia-Muñoz *et al.,* Phys. Rev. B **55**, 34 (1997).
[11] J. D. Lee and B. I. Min, Phys. Rev. B **55**, 12 454 (1997); Unjong Yu, B. I. Min, and J. D. Lee, Phys. Rev. B **61**, 84 (2000).
[12] K. H. Kim *et al.,* Phys. Rev. Lett. **77**, 1877 (1996).
[13] S. Yoon *et al.,* Phys. Rev. B **58**, 2795 (1998).
[14] E. Liarokapis *et al.,* Phys. Rev. B **60**, 12 758 (1999).
[15] M. N. Iliev *et al.,* Phys. Rev. B **57**, 2872 (1998).
[16] V. Dediu *et al.,* Phys. Rev. Lett. **84**, 4489 (2000).
[17] D. Levy, C. Meneghini, S. Mobilio, A. Kumar, and D. D. Sarma (unpublished).
[18] C. Meneghini *et al.,* Phys. Status Solidi **215**, 647 (1999); C. Meneghini, C. Castellano, S. Mobilio, A. Kumar, S. Ray, and D. D. Sarma (to be published).
[19] H. K. Mao *et al.,* J. Appl. Phys. **49**, 3276 (1978).
[20] A. Congeduti, P. Postorino, and M. Nardone (unpublished).
[21] Y. Moritomo *et al.,* Nature (London) **380**, 141 (1996).
[22] V. B. Podobedov *et al.,* Phys. Rev. B **58**, 43 (1998).
[23] A. V. Boris *et al.,* Phys. Rev. B **59**, R697 (1999).
[24] E. Granado *et al.,* Phys. Rev. B **60**, 11 879 (1999).